THE JOURNAL OF BIOLOGICAL CHEMISTRY VOL. 289, NO. 31, pp. 21423–21432, August 1, 2014

Sec23 Homolog Nel1 Is a Novel GTPase-activating Protein for Sar1 but Does Not Function as a Subunit of the Coat Protein Complex II (COPII) Coat*

Received for publication, January 29, 2014, and in revised form, June 8, 2014 Published, JBC Papers in Press, June 19, 2014, DOI 10.1074/jbc.M114.553917

Chie Kodera[‡], **Tomohiro Yorimitsu**[§], **and Ken Sato**[‡§1]

From the [‡]*Department of Biological Sciences, Graduate School of Science, University of Tokyo, Hongo, Bunkyo-ku, Tokyo 113-0033 and the* [§]*Department of Life Sciences, Graduate School of Arts and Sciences, University of Tokyo, Komaba, Meguro-ku, Tokyo 153-8902, Japan*

Background: Sec23 is a COPII coat subunit involved in ER-to-Golgi trafficking under the control of the Sar1 GTPase.
Results: The Sec23 homolog Nel1 has genetic and biochemical interactions with Sar1 but is not part of the COPII complex.
Conclusion: Nel1 is a novel Sec23 paralog that shows a functional link with Sar1.
Significance: Nel1 is the first Sar1-GAP demonstrated to not function as a subunit of the COPII coat.

The coat protein complex II (COPII) generates transport carriers from the endoplasmic reticulum (ER) under the control of the small GTPase Sar1. Sec23 is well known as a structural component of the COPII coat and as a GTPase-activating protein (GAP) for Sar1. Here, we showed that *Saccharomyces cerevisiae* contains a novel Sec23 paralog, Nel1, which appears not to function as a subunit of the COPII coat. Nel1 does not associate with any of the COPII components, but it exhibits strong Sar1 GAP activity. We also demonstrated that the chromosomal deletion of *NEL1* leads to a significant growth defect in the temperature-sensitive *sar1D32G* background, suggesting a possible functional link between these proteins. In contrast to Sec23, which is predominantly localized at ER exit sites on the ER membrane, a major proportion of Nel1 is localized throughout the cytosol. Our findings highlight a possible role of Nel1 as a novel GAP for Sar1.

In eukaryotic cells, newly synthesized membrane and soluble proteins in the endoplasmic reticulum (ER)[2] destined for export to the Golgi or beyond are concentrated at specialized ER exit sites (ERES), where they are packaged into transport carriers generated by COPII coat proteins (1–3). The COPII coat consists of an inner layer of the Sec23/24 heterodimeric complex surrounded by an outer layer of the Sec13/31 heterotetramer complex, and these components are sequentially assembled onto the ER membrane through the action of the small GTPase Sar1 (4–6). In brief, the assembly of the COPII coat is triggered by a GDP-GTP exchange on Sar1 that is catalyzed by the ER-resident guanine nucleotide exchange factor Sec12 (7, 8). The activated Sar1-GTP binds to the ER membranes and recruits the Sec23/24 complex by binding to the Sec23 portion, and the Sec24 subunit captures the cargo protein to form a prebudding complex (9–11). Subsequently, the outer layer of the Sec13/31 complex is recruited onto Sec23/24, which polymerizes adjacent prebudding complexes to drive membrane deformation (12, 13). The Sec23 subunit is the GTPase-activating protein (GAP) for Sar1, and repeated cycles of Sec12-dependent GTP loading to Sar1 and Sec23-mediated hydrolysis facilitate proper and efficient cargo sorting into COPII vesicles (14–17). Thus, Sec23 acts both as a component of the COPII coat structure and as the GAP for the small GTPase Sar1, as well as regulating COPII assembly. Recent findings have suggested that GTPase inhibitory activity mediated by the peripheral membrane protein Sec16 also modulates the assembly of the COPII coat at ERES (18, 19).

In humans and many other species, gene duplication events generate multiple paralogs for most of these COPII components (20). However, it is not clear whether these COPII paralogs are functionally redundant or whether their multiplication represents an adaptation to either the increased complexity of cargo proteins or to the tissue-specific requirements. Although most eukaryotes carry two paralogs of Sec23 (21), no Sec23 paralogs have been described in *Saccharomyces cerevisiae* to date. In this study, we show that *S. cerevisiae* contains a novel Sec23 paralog that we designated Nel1 (non-ERES-localized Sec23 homolog 1), which appears to have a function distinct from that of Sec23. We found that purified Nel1 activates the GTPase activity of Sar1 but does not associate with any of the COPII coat components. Nel1 is predominantly localized throughout the cytosol, and the chromosomal disruption of *NEL1* affects the growth phenotype of the temperature-sensitive *sar1* mutant. Our findings provide a possible functional link between Sar1 and its novel GAP, Nel1.

* This work was supported in part by grant-in-aid for scientific research (C), grant-in-aid for scientific research on innovation areas "Supramolecular Motility Machinery" and "Dynamical Ordering of Biomolecular Systems for Creation of Integrated Functions" from the Ministry of Education, Culture, Sports, Science and Technology, the Naito Foundation, the Kurata Memorial Hitachi Science and Technology Foundation, and the Noda Institute for Scientific Research.

[1] To whom correspondence should be addressed: Dept. of Biological Sciences, Graduate School of Science, University of Tokyo, Hongo, Bunkyo-ku, Tokyo 113-0033, Japan. Tel.: 81-3-5454-6749; Fax: 81-3-5454-6730; E-mail: kensato@bio.c.u-tokyo.ac.jp.

[2] The abbreviations used are: ER, endoplasmic reticulum; ERES, ER exit site; MBP, maltose-binding protein; COPII, coat protein complex II; GAP, GTPase-activating protein; GMP-PNP, guanosine-5′-[(β,γ)-imido]triphosphate.

TABLE 1
Yeast strains used in this study

Strain	Genotype	Ref.
ANY21	*MAT*a *ura3-52 leu2-3,112 trp1-289 his3 his4 suc gal2*	7
CKY1	*MAT*a *nel1*Δ*::LEU2 ura3-52 leu2-3,112 trp1-289 his3 his4 suc gal2*	This study
CKY2	*MAT*a *nel1*Δ*::LEU2 sar1*Δ*::HIS3 pep4::ADE2 ura3 leu2 trp1 his3 ade2 lys2*/pMYY3-l (YCp (SAR1 *TRP1*)	This study
CKY3	*MAT*α *nel1*Δ*::LEU2 sar1*Δ*::HIS3 pep4::ADE2 ura3 leu2 trp1 his3 ade2 lys2* / pMYY3-7 (YCp (*sar1D32G TRP1*))	This study
MBY8-20C	*MAT*a *sec23-1 ura3-52 leu2-3,112 trp1-289 his3 his4*	Bernstein and Schekman[a]
PJ69-4A	*MAT*a *trp1-901 leu2-3,112 ura3-52 his3-200 gal4*Δ *gal80*Δ *GAL2-ADE2 LYS2::GAL1-HIS3 met2::GAL7-lacZ*	24
TOY221	*MAT*a *sar1*Δ*::HIS3 pep4::ADE2 ura3 leu2 trp1 his3 ade2 lys2*/pMYY3-l (YCp (SAR1 *TRP1*))	23
TOY223	*MAT*α *sar1*Δ*::HIS3 pep4::ADE2 ura3 leu2 trp1 his3 ade2 lys2*/pMYY3-7 (YCp (*sar1D32G TRP1*))	23
YPH500	*MAT*α *ura3-52 lys2-801_amber ade2-101_ochre trp1-*Δ*63 his3-*Δ*200 leu2-*Δ*1*	Sikorski and Hieter[b]

[a] Bernstein and R. Schekman, unpublished data.
[b] Sikorski and Hieter, unpublished data.

EXPERIMENTAL PROCEDURES

Strains and Media—The strains used in this study are listed in Table 1. Gene deletions were performed by a PCR-based procedure using the plasmid pUG73 as a template (22). CKY1, CKY2, and CKY3 were generated from ANY21 (7), TOY221, and TOY223 (23), respectively. Unless otherwise noted, the cultures were grown at 30 °C in YPD medium (1% Bacto-yeast extract, 2% polypeptone, and 2% dextrose), MVD medium (2% dextrose and 0.67% yeast nitrogen base without amino acids), MCD medium (0.67% yeast nitrogen base without amino acids, 0.5% casamino acids, and 2% dextrose), or MCGS medium (0.67% yeast nitrogen base without amino acids, 0.5% casamino acids, 5% galactose, and 0.2% sucrose) supplemented appropriately.

Plasmid Construction—The coding sequences of the *NEL1* gene or the *SEC23* gene, together with its upstream and downstream flanking regions, were amplified by PCR using the *Saccharomyces cerevisiae* genomic DNA and inserted into the NotI and BamHI (*NEL1*) or the BamHI and SalI (*SEC23*) sites of pRS316 (*CEN*, *URA3*), yielding pNEL1/316 and pSEC23/316, respectively. A fragment, including the *TDH3* promoter and *CMK1* terminator, was inserted into the BamHI and SalI sites of pRS316, pYO326 (2μ, *URA3*), pYO324 (2μ, *TRP1*), and pRS314 (*CEN*, *TRP*), yielding pCKY4, pCKY5, pCKY6, and pCKY8, respectively. The coding sequences of the *NEL1* and *SEC23* genes were amplified by PCR from yeast genomic DNA and inserted into the BglII site (located between *TDH3* promoter and *CMK1* terminator) of pCKY5, yielding pNEL1/CKY5 and pSEC23/CKY5, respectively. To generate plasmids for yeast two-hybrid analysis, *NEL1* was cloned into the BglII sites of pGAD-C1 and pGBDU-C1 (24). *SEC24*, which was digested with SmaI and XhoI, was cloned into the SmaI and SalI sites of pGAD-C1 and pGBDU-C1. *SEC23*, *LST1*, and *ISS1* were cloned into the BamHI and SalI, EcoRI and BamHI, and BamHI and PstI sites, respectively, of pGAD-C1. For Nel1-MBP purification, the coding sequence of *NEL1* together with a Myc tag at the N terminus and an SphI site just before the stop codon was amplified by PCR from yeast genomic DNA and inserted into the BglII site of pCKY6, and a fragment encoding MBP, amplified by PCR from pMAL-c2x (New England Biolabs), was inserted into the SphI site, yielding pNEL1-MBP/CKY6. For Nel1-R592A-MBP purification, the R592A mutation was introduced into pNEL1-MBP/CKY6 by primer-directed mutagenesis, yielding pNEL1-R592A-MBP/CKY6. For pulldown assay, plasmids expressing Sec24-HA, Lst1-HA, or Iss1-HA under the *GAL* promoter were obtained from yeast ORF collection (Open Biosystems). A fragment encoding MBP together with a Myc tag at the N terminus was amplified by PCR from pMAL-c2x and inserted into the BglII site of pCKY8, yielding pMBP/CKY8. The coding sequence of *SEC23* together with a Myc tag at the N terminus and an XmaI site just before the stop codon were amplified by PCR from yeast genomic DNA and inserted into the SacI and XhoI sites of pYES3/CT (Invitrogen), and a fragment encoding MBP, amplified by PCR from pMAL-c2x, was inserted into the XmaI site, yielding pSEC23-MBP/YES3. To obtain the plasmid pNEL1–13Myc/316, we first generated a yeast strain CKY4 by a PCR-based procedure using pFA6a-13Myc-TRP1 (25), which chromosomally expresses C-terminally 13Myc-tagged Nel1. The coding sequence of the Nel1–13Myc, together with its upstream and downstream flanking regions, was amplified by PCR from the genome of the CKY4 strain and inserted into the NotI and BamHI sites of pRS316, yielding pNEL1–13Myc/316. The fragment encoding enhanced GFP was inserted into the BglII and HindIII sites of pCKY4, yielding pCKY7. The coding region of *NEL1*, amplified by PCR from yeast genomic DNA, was inserted into the BglII site of pCKY7, yielding pNEL1/CKY7. The coding sequences of the *NEL1* and *HTB1* genes, together with their upstream and downstream flanking regions, were amplified by PCR from yeast genomic DNA and inserted into the NotI and BamHI (*NEL1*) and NotI and XhoI (*HTB1*) sites of pRS314 (*CEN*, *TRP1*), yielding pNEL1/314 and pHTB1/314, respectively. For the fluorescent protein fusions, SphI (*NEL1*) and BamHI (*HTB1*) sites were created just before the stop codon of each gene. Then, fragments encoding mCherry and AcGFP (Clontech) were inserted into the SphI (Nel1-mCherry) and BamHI (Htb1-GFP) sites, yielding pNEL1-mCherry/314 and pHTB1-GFP/314, respectively. A fragment encoding NEL1-mCherry, amplified by PCR from pNEL1-mCherry/314, was then inserted into the BglII site of pCKY4, yielding pNEL1-mCherry/CKY4.

Protein Preparation—Sar1, Sec23/24, and Sec13/31 were purified as described previously (6, 26). Nel1-MBP and Nel1-R592A-MBP were purified from yeast YPH500 cells carrying the pNEL1-MBP/CKY6 or pNEL1-R592A-MBP/CKY6 plasmids, respectively. The cells were grown to late-log phase at 30 °C. The cells from 12 liters of cultures were washed with distilled water and then resuspended in suspension buffer (50 mM HEPES-KOH, pH 7.4, 500 mM KoAc, 5 mM EDTA, 10% glycerol) containing a 3× protease inhibitor mixture (Roche Applied Science). The cell suspension was frozen as drops by pouring it into liquid nitrogen and then stored at −80 °C. The

frozen cells were subsequently blended and thawed on ice. From the supernatant obtained from a 20-min centrifugation at 9,500 rpm with a JA-14 rotor (Beckman Coulter) at 4 °C, the protein extract was recovered by ultracentrifugation at 42,000 rpm for 1 h at 4 °C in a Hitachi P45AT rotor. The supernatant was incubated with amylose resin (New England Biolabs) for 1.5 h at 4 °C. The resin was washed with wash buffer 1 (20 mM HEPES-KOH, pH 7.4, 500 mM KoAc, 5 mM EDTA, 10% glycerol) and then with wash buffer 2 (20 mM HEPES-KOH, pH 7.4, 500 mM KoAc, 1 mM EDTA, 10% glycerol). Nel1-MBP and Nel1-R592A-MBP were eluted with elution buffer (20 mM HEPES-KOH, pH 7.4, 500 mM KoAc, 50 mM maltose, 10% glycerol).

Pulldown Assay—YPH500 cells carrying the appropriate plasmids were pregrown to mid-log phase at 30 °C in MCD medium and then transferred to MCGS medium. After a 2.5-h incubation, 20 absorbance units of cells (per sample) were harvested and resuspended in suspension buffer (20 mM HEPES-KOH, pH 7.4, 500 mM KoAc, 5 mM EDTA, 10% glycerol). The cells were disrupted by vortex mixing with glass beads at 4 °C, and protein extracts were incubated with amylose resin for 1 h at 4 °C. The resins were washed with the suspension buffer, and samples were eluted by elution buffer (20 mM HEPES-KOH, pH 7.4, 500 mM KoAc, 50 mM maltose, 10% glycerol). The samples were then analyzed by SDS-PAGE and immunoblotting.

Tryptophan Fluorescence Measurements and Liposome Binding Assay—Tryptophan fluorescence measurements and liposome binding assays were carried out as described previously (15, 17). All experiments were performed with synthetic major-minor mix liposomes (27).

Fluorescence Microscopy—Yeast cells expressing fluorescent proteins were grown to mid-log phase at 23 °C. Fluorescence microscopy observations were carried out using an Olympus IX71 microscope equipped with a CSU10 spinning-disk confocal scanner (Yokogawa Electric Corp.) and an electron-multiplying charge-coupled device camera (iXon, DV897; Andor Technology). The acquired images were analyzed using Andor iQ (Andor Technology). In this setting, a 473-nm solid-state laser (J050BS; Showa Optronics) was used to excite AcGFP, enhanced GFP, and mCherry at 561 nm (Jive; Cobolt).

Subcellular Fractionation—Subcellular fractionation was performed as described previously (28). In brief, CKY1 cells carrying pNEL1–13Myc/316 were grown to mid-log phase, and 500 absorbance units of cells (per sample) were converted to spheroplasts by treatment with Zymolyase. The spheroplasts were resuspended in 2× lysis buffer (40 mM HEPES-KOH, pH 7.4, 400 mM sorbitol, 100 mM KoAc, 4 mM EDTA, supplemented with protease inhibitor mixture and 1 mM DTT) and then centrifuged at 3,000 rpm for 10 min in a Beckman JA-14 rotor. The spheroplast pellets were resuspended in lysis buffer (20 mM HEPES-KOH, pH 7.4, 200 mM sorbitol, 50 mM KoAc, 2 mM EDTA, supplemented with protease inhibitor mixture and 1 mM DTT) and then subjected to seven strokes in a Dounce homogenizer. The lysates were centrifuged at 300 × *g* for 5 min to remove unbroken materials, yielding the total fractions (S3). The total fractions were centrifuged at 13,000 × *g* for 15 min to generate the S13 supernatants and P13 pellets. The P13 pellets were washed four times with lysis buffer. The samples were then analyzed by SDS-PAGE and immunoblotting.

RESULTS

NEL1, a Gene Encoding a Sec23-like Protein—A search of the yeast *S. cerevisiae* genome revealed an uncharacterized open reading frame, YHR035W, that encodes a 630-amino acid nonessential protein with sequence similarity to members of the Sec23 family, which we designated Nel1. Alignment analysis using ClustalX revealed that Nel1 has strong similarity to Sec23, with 21% identity and 37% similarity. Nel1 contains a putative catalytic arginine residue (Arg-592) necessary for the GAP activity on Sar1 (Fig. 1) (9).

Given the sequence similarity of Nel1 to Sec23, we first examined whether Nel1 could complement the temperature sensitivity of a *sec23-1* mutant (29). Because *sec23-1* cells already have a chromosomal copy of *NEL1*, endogenous expression of Nel1 is clearly not sufficient to rescue the temperature-sensitive phenotype of the *sec23-1* strain. However, even high copy expression of Nel1 under the control of a strong constitutive *TDH3* promoter could not suppress the temperature-sensitive growth defect of the *sec23-1* mutant (Fig. 2*A*). In addition, overexpression of Nel1 was not found to have obvious effects on growth of the other early *sec* mutants tested (*sar1D32G*, *sar1E112K*, *sar1N132I*, *sec12-4*, *sec13-1*, or *sec16-2*) (data not shown). A previous study has shown that overexpression of Sec23 leads to growth inhibition in wild-type cells, presumably by disturbing the GDP/GTP cycling of Sar1 through the excess GAP activity of Sec23 (30). However, overexpression of Nel1 did not cause any apparent growth defect in wild-type cells (Fig. 2*B*). The combined results suggest that Nel1 activity is not functionally redundant with Sec23, thus suggesting a specialized role(s) for this protein *in vivo*.

Nel1 Does Not Associate with Sec24 and Its Homologs—In *S. cerevisiae* and higher eukaryotes, Sec23 forms a stable complex with either Sec24 or its closely related homologs (9). We therefore determined whether Nel1 could also associate with Sec24 and its yeast homologs, Lst1 or Iss1 (30–32). As revealed by a yeast two-hybrid assay, Sec23 indeed associated with Sec24, whereas no interactions were observed between Nel1 and Sec24, Lst1, or Iss1 (Fig. 2*C*). To further confirm the two-hybrid results, we performed pulldown experiments in lysates prepared from yeast cells expressing both Nel1 tagged C-terminally with an MBP tag (Nel1-MBP) and HA-tagged Sec24, Lst1, or Iss1. As shown in Fig. 2*D*, we observed that Nel1-MBP was not able to pull down Sec24, Lst1, or Iss1, whereas Sec23-MBP formed complexes with Sec24 and its isoforms. Indeed, SDS-PAGE analysis of the affinity-purified Nel1-MBP fusion protein revealed that additional components did not copurify with Nel1-MBP (Fig. 3*A*). Consistent with these findings, the residues in Sec23 involved in the intersubunit interactions between Sec23 and Sec24 are poorly conserved in Nel1 (Fig. 1) (9). These results suggest that, unlike Sec23, Nel1 may not associate with Sec24 and its homologs.

Nel1 Has GAP Activity toward Sar1—Despite the absence of a detectable interaction with Sec24 and its homologs, Nel1 contains a region with sequence homology to the C-terminal domain of Sec23, which includes a crucial arginine residue

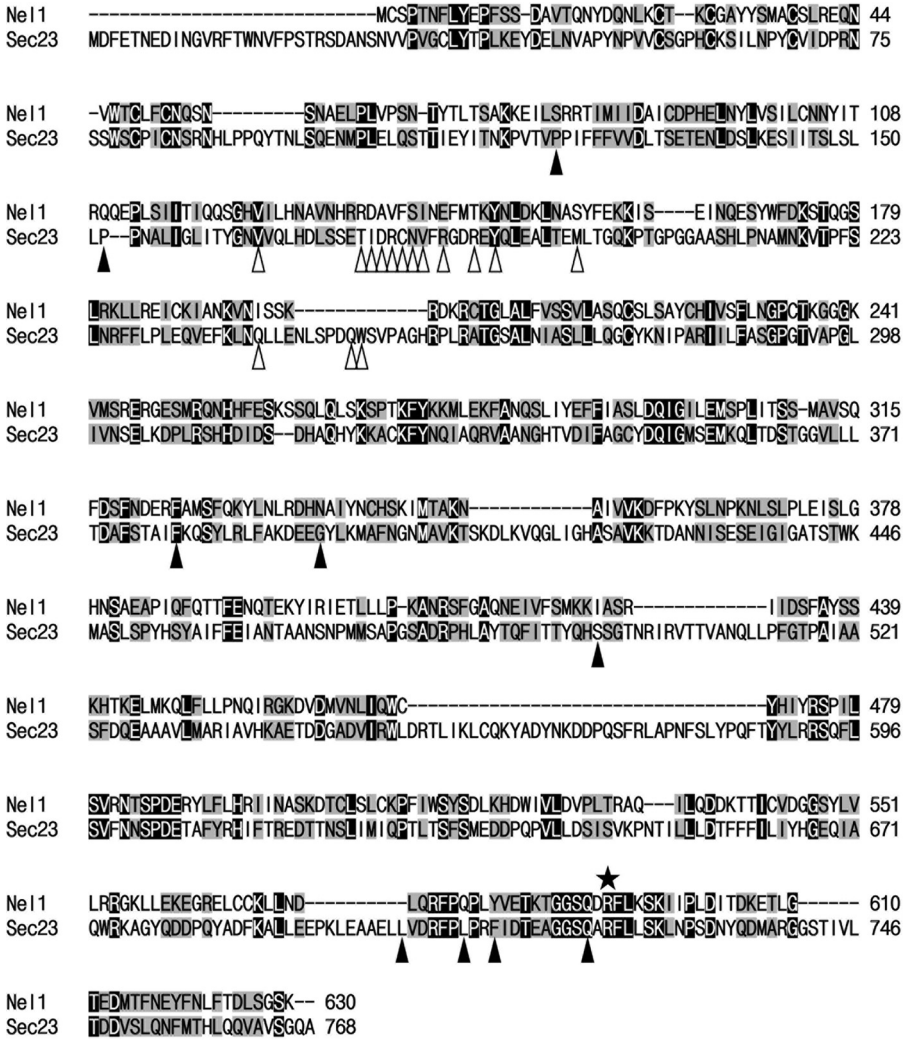

FIGURE 1. **Pairwise sequence alignment of Sec23 and its closest paralog, YHR035W.** The optimal alignment was obtained by using the ClustalX program. Highlighted residues (*white letters* on *black*) indicate amino acids that are identical to those of Sec23, and *gray residues* indicate conservation. The *star* indicates the catalytic arginine residue necessary for Sec23 GAP activity. *Arrowheads* indicate residues making intersubunit interactions between Sec23/Sec24 (*white*) and Sec23/Sec31 (*black*).

required for Sec23 GAP activity (Fig. 1) (9). The corresponding arginine residue is also conserved in Nel1 (Arg-592), which suggests that Nel1 may also have GAP activity toward Sar1. To examine whether Nel1 affects Sar1 GTPase activity, affinity-purified Nel1-MBP was tested for GAP activity on Sar1 by using a real time tryptophan fluorescence assay (15, 17). We incubated liposomes ("major-minor mix" lipids, previously established as the optimal composition for COPII recruitment) (27) preloaded with Sar1-GTP and monitored the decrease in the intrinsic tryptophan fluorescence of Sar1 that accompanies the conversion of Sar1 from the GTP state to the GDP state after the addition of Nel1-MBP or control Sec23/24 (Fig. 3*B*). As expected, the addition of Nel1-MBP markedly accelerated the GTPase activity of Sar1. At an equal molar concentration, Nel1 was ~5-fold (in arbitrary units) more potent than Sec23/24 at promoting GTP hydrolysis on Sar1. Replacement of the arginine 592 residue of Nel1 with alanine (Nel1-R592A-MBP) virtually abolished Nel1's GAP activity, indicating the direct involvement of this residue in catalysis. We also examined the effect of Nel1-R592A overexpression on the growth of the wild-type strain and observed no detectable alternation in growth rate (Fig. 2*B*), suggesting that Nel1 GAP activity is not directly involved in normal cell growth.

We next determined whether the GAP activity of Nel1 could be further accelerated by Sec13/31, as has been observed with Sec23 (15). However, the presence of Sec13/31 did not substantially influence the GAP activity of Nel1 (Fig. 3*C*). Assembly of the COPII coat proceeds in a stepwise manner by the recruitment of Sar1-GTP, which binds to the lipid surface, followed by association of Sec23/24 and Sec13/31. This process has been reconstituted *in vitro* using synthetic liposomes (27). We tested the ability of Nel1 to bind to liposomes loaded with Sar1 and whether it could in turn recruit Sec13/31 in this reconstituted system. Liposomes were incubated with different combinations of the COPII coat proteins as indicated in Fig. 3*D*, followed by flotation on a sucrose density gradient. Similar to Sec23/24, Nel1 bound to these liposomes in a Sar1- and GMP-PNP-dependent manner, but the subsequent recruitment of Sec13/31 was not observed. Therefore, the complete loss of the ability of Sec13/31 to stimulate the GAP activity of Nel1 is likely to be due

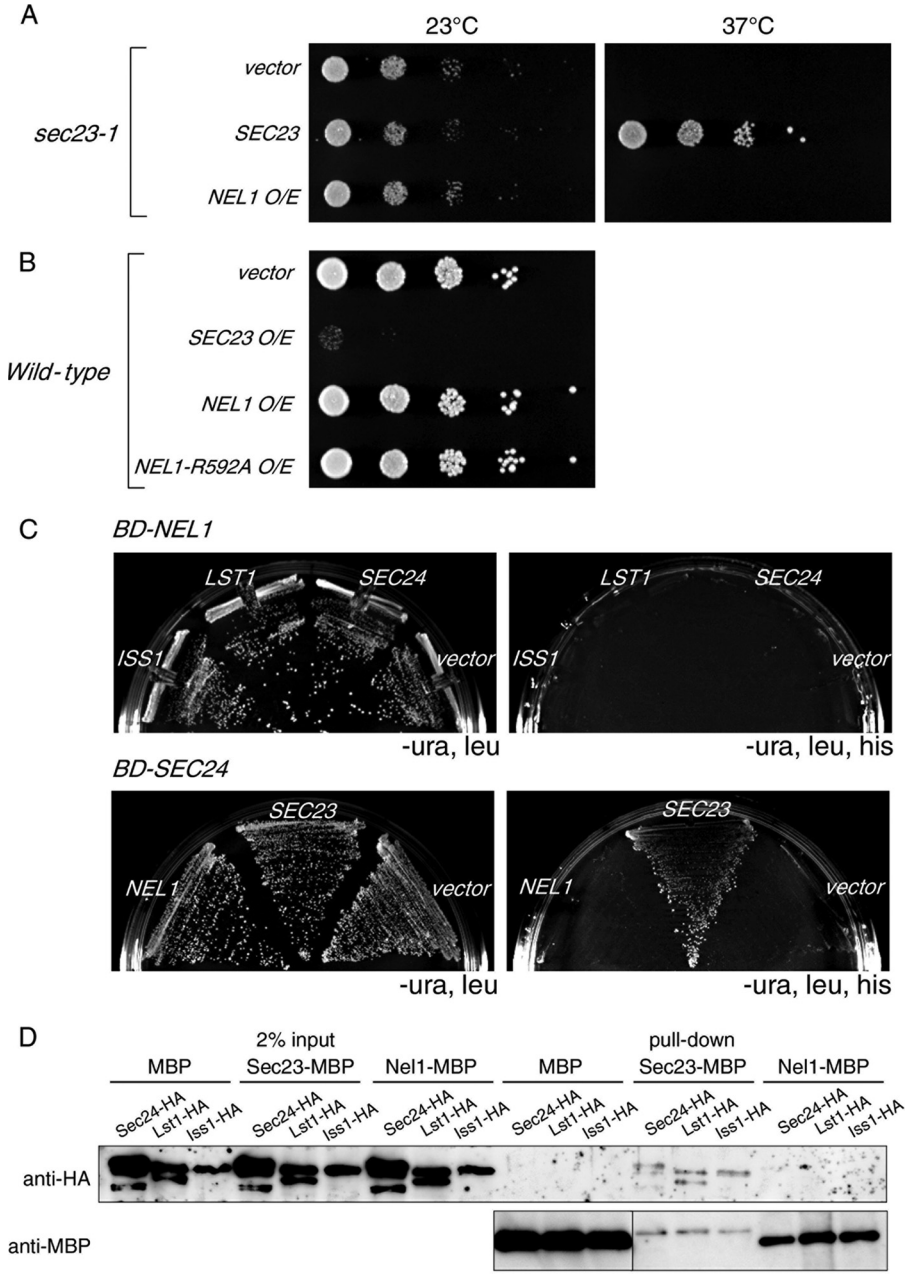

FIGURE 2. **Nel1 has a function distinct from that of Sec23.** *A,* Nel1 overexpression cannot compensate for the loss of Sec23 function. The *sec23-1* cells were transformed with pCKY5 (2μ vector), pNEL1/CKY5 (2μ *NEL1*), or pSEC23/316 (*CEN SEC23*). The *SEC23* gene was expressed from its own promoter on a single-copy plasmid because overexpression of Sec23 is toxic. The transformants were grown to saturation at 23 °C and adjusted to an A_{600} of 0.3. Then, 5 μl of a 10-fold dilution series were spotted onto selective plates and incubated at the indicated temperatures. *B,* Nel1 overexpression does not lead to a growth defect. Wild-type (ANY21) cells transformed with pCKY5 (2μ vector), pSEC23/CKY5 (2μ *SEC23*), or pNEL1/CKY5 (2μ *NEL1*) were grown to saturation at 30 °C and then adjusted to an A_{600} of 0.3. Then 5 μl of a 10-fold dilution series were spotted onto selective plates and incubated at 30 °C. *A* and *B, O/E* indicates overexpression. *C,* Nel1 does not associate with Sec24 and its homologs, as revealed by a yeast two-hybrid assay. The PJ69-4A strain was transformed with plasmids containing the binding domain-fused Nel1 and activation domain-fused Sec24, Lst1, or Iss1, and transformants were grown on plates lacking histidine at 30 °C (*upper panel*). The PJ69-4A strain was transformed with plasmids containing binding domain-fused Sec24 and activation domain-fused Nel1 or Sec23, and transformants were grown on plates lacking histidine at 30 °C (*lower panel*). *D,* Nel1 does not associate with Sec24 and its homologs, as revealed by MBP pulldown assays. Cells expressing indicated proteins were lysed and subjected to pulldown assay with the indicated MBP fusion proteins, and bound proteins were analyzed by SDS-PAGE and immunoblotting. *A–D,* results shown are typical and representative of at least three independent experiments.

to the fact that Nel1 is not active in the recruitment of Sec13/31. Consistent with these findings, the residues in Sec23 involved in the intersubunit contacts with Sec31 are poorly conserved in Nel1 (Fig. 1) (12). To compare the relative affinities of Sec23 and Nel1 for Sar1, we quantified the binding efficiencies of these two proteins to Sar1 in Fig. 3*D*. The binding levels relative to the amount of membrane-bound Sar1 were similar for both Sec23 (0.0037 ± 0.0018) and Nel1 (0.0034 ± 0.00043) (Fig. 3*E*), indicating that the Nel1 has roughly equal affinity for Sar1 as Sec23. We also confirmed that Nel1-R592A-MBP can bind to Sar1-GMP-PNP, ensuring that this mutant protein was properly folded (Fig. 3*F*). Furthermore, the fact that Nel1-R592A-MBP can bind Sar1, but exhibits no GAP activity, excludes the possibility that tryptophan residues in Nel1 somehow contrib-

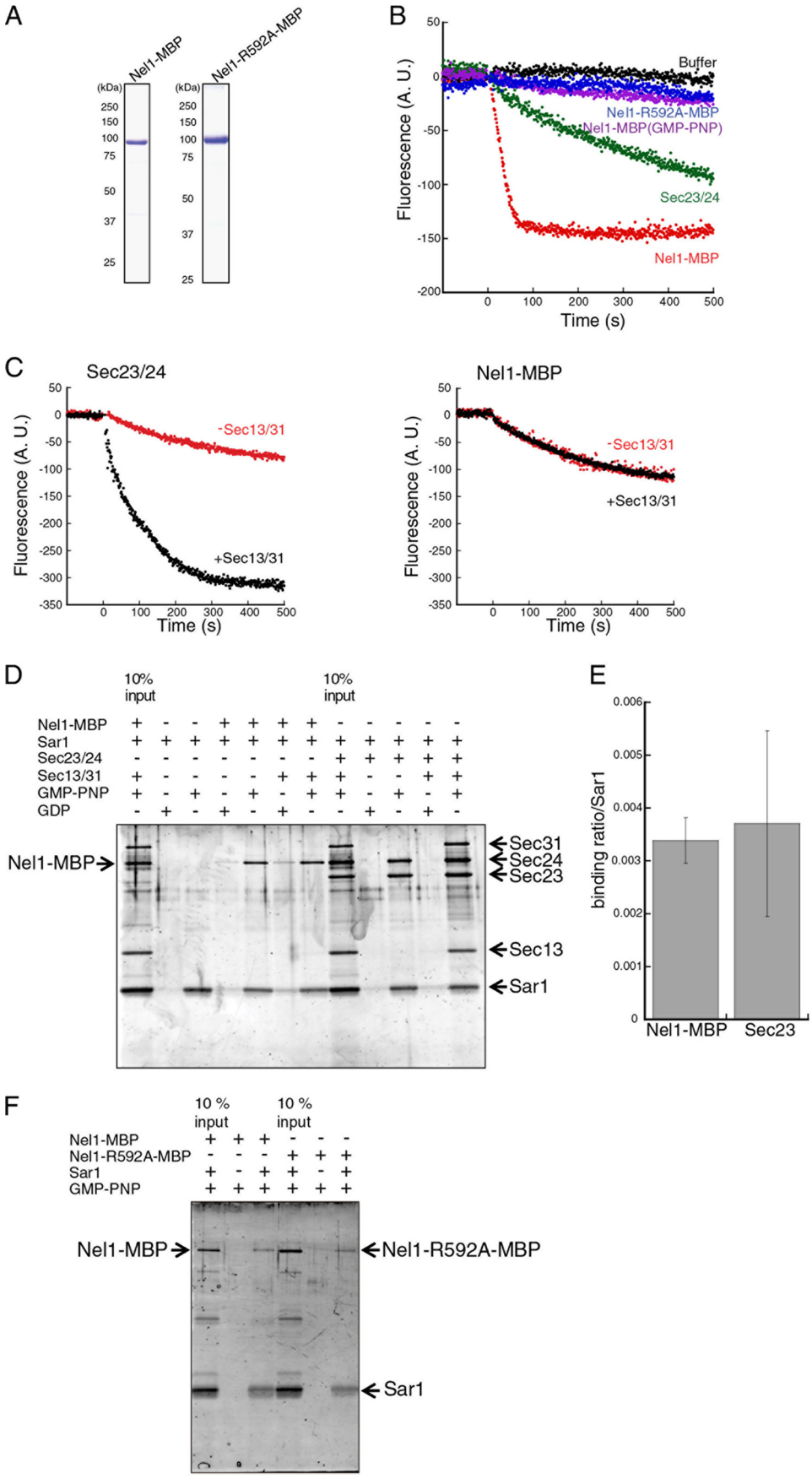
A
Nel1-MBP
Nel1-R592A-MBP
(kDa)
250
150
100
75
50
37
25
B
Fluorescence (A. U.)
Time (s)
Buffer
Nel1-R592A-MBP
Nel1-MBP(GMP-PNP)
Sec23/24
Nel1-MBP
C
Sec23/24
Nel1-MBP
-Sec13/31
+Sec13/31
Fluorescence (A. U.)
Time (s)
D
10% input
Nel1-MBP
Sar1
Sec23/24
Sec13/31
GMP-PNP
GDP
Nel1-MBP
Sec31
Sec24
Sec23
Sec13
Sar1
E
binding ratio/Sar1
Nel1-MBP
Sec23
F
10 % input
Nel1-MBP
Nel1-R592A-MBP
Sar1
GMP-PNP
Nel1-MBP
Nel1-R592A-MBP
Sar1

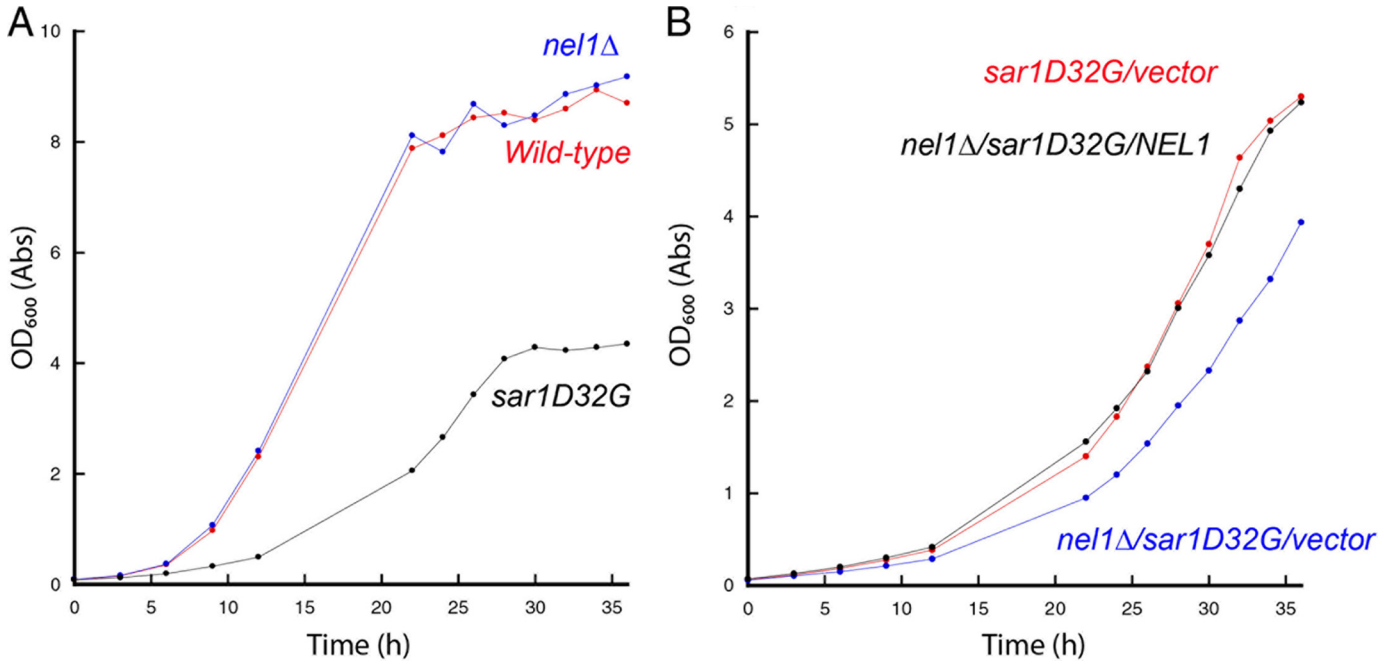

FIGURE 4. ***NEL1* has a genetic interaction with *SAR1*.** *A,* growth phenotype of the *nel1*Δ strain. Wild-type (TOY221), *nel1*Δ (CKY2), and *sar1D32G* (TOY223) cells were cultured at 23 °C overnight and adjusted to an A_{600} of 0.1 in YPD medium, Then the cultures were analyzed for growth at 23 °C over time by absorbance at 600 nm. *B, sar1D32G/nel1*Δ double mutant has a synthetic growth defect. The *sar1D32G* (TOY223) and *sar1D32G/nel1*Δ (CKY3) cells carrying the indicated plasmids were analyzed as in *A*. *A* and *B,* results shown are typical and representative of at least three independent experiments.

ute to the change in fluorescence that occurs upon incubation with Sar1-GTP, as observed in Fig. 3*B*. We concluded from these kinetic and biochemical results that Nel1 has some role in the regulation of Sar1 GTPase activity but may have a function distinct from that of Sec23 as a subunit of the COPII vesicle coat.

Chromosomal Disruption of NEL1 in Combination with sar1D32G Mutation Exhibits a Slow Growth Phenotype—To obtain evidence of a functional relationship between Sar1 and Nel1 *in vivo*, we examined genetic interactions between the genes (Fig. 4). To this end, the temperature-sensitive *sar1D32G* allele was combined with the *nel1*Δ mutation, and the ability of this mutant to grow at the permissive temperature (23 °C) was assessed. The single *nel1*Δ mutant cells grew identically to wild-type cells, whereas the growth of the *sar1D32G* mutant was much slower even at the permissive temperature as reported previously (Fig. 4*A*) (33). The growth rate was further impaired in the *sar1D32G*/*nel1*Δ double mutant (Fig. 4*B*). This growth defect of the *sar1D32G*/*nel1*Δ strain could be restored by introduction of a plasmid carrying the *NEL1* gene (Fig. 4*B*). These observations indicate that combining the *sar1D32G* and *nel1*Δ mutations causes a synthetic growth defect and thus provide strong genetic support for a possible functional link between Sar1 and Nel1. We also confirmed that the tagged versions of Nel1 (Nel1–13Myc, Nel1-mCherry, and Nel1-GFP) were fully functional by observing complementation of the growth defect of a *sar1D32G*/*nel1*Δ strain (data not shown).

Subcellular Localization of Nel1—COPII coat proteins, including Sec23, are predominantly localized to punctate structures at ERES on the ER membrane (34, 35). We next sought to determine the subcellular localization of Nel1-GFP expressed under its own promoter, but the expression was found to be below the limit of detection. Nel1 fusions that contained two or even three tandem repeats of the GFP moiety showed the same result, suggesting that this protein is expressed at much lower levels than Sec23 (data not shown). We therefore examined the localization of overexpressed Nel1-GFP or Nel1-mCherry (Fig. 5, *A* and *B*). In sharp contrast with its homolog Sec23, the fluorescence for Nel1 was diffusely localized throughout the cytosol, and we could not observe any ERES-like punctate structures. In addition, Nel1 was also found in the nucleus, as evidenced by its colocalization with the nuclear marker Htb1-

FIGURE 3. **Nel1 has strong GAP activity toward Sar1 but does not recruit Sec13/31.** *A,* Nel1-MBP and Nel1-R592A-MBP were purified from yeast cells. Proteins from YHP500 cells expressing Nel1-MBP or Nel1-R592A-MBP were purified by amylose resin, and they were separated by SDS-PAGE followed by staining with Coomassie Brilliant Blue. *B,* Nel1 accelerates GTP hydrolysis by Sar1. The reaction initially contained liposomes (100 μg/ml), Sar1 (800 nM), and GTP or GMP-PNP (0.1 mM). After preincubation, Nel1-MBP, Nel1-R592A-MBP, or Sec23/24 (15 nM) was added at 0 s. Transition of Sar1 from the GTP-bound to the GDP-bound state was monitored by tryptophan fluorescence of Sar1 at 340 nm. *C,* Sec13/31 does not stimulate Nel1-mediated GAP activity on Sar1. The reaction initially contained liposomes (100 μg/ml), Sar1 (800 nM), and GTP (0.1 mM). After preincubation, Sec23/24 (15 nM) and Sec13/31 (22.5 nM) (*left panel*) or Nel1-MBP (5 nM) and Sec13/31 (5 nM) (*right panel*) were added at 0 s, and the Sar1-GTP to Sar1-GDP transition was monitored by tryptophan fluorescence of Sar1 at 340 nm. *D,* liposome binding assays of COPII proteins with Nel1. Sar1 (800 nM), Sec13/31 (200 nM), Nel1-MBP or Sec23/24 (120 nM) were incubated with GDP or GMP-PNP (0.1 mM) in the presence of synthetic liposomes (100 μg/ml) and subjected to flotation on a sucrose density gradient. Float fractions were then subjected to SDS-PAGE and stained with SYPRO Orange. *E,* quantification of the binding efficiencies of Sec23 and Nel1-MBP for Sar1. The band intensities of Sec23 or Nel1 in *D* were normalized to those of Sar1, and the values of Sar1-bound Sec23 (or Nel1-MBP)/total input Sec23 (or Nel1-MBP) were calculated. The means ± S.D. are shown in the *graph*. These results were verified by applying Student's *t* test. *p* value was >0.1. *F,* liposome binding assays of Nel1-R592A. Sar1 (800 nM), Nel1-MBP (120 nM), or Nel1-R592A-MBP (120 nM) were incubated with GMP-PNP (0.1 mM) in the presence of synthetic liposomes (100 μg/ml) and subjected to flotation as in *D*. *B–D* and *F,* results shown are typical and representative of at least three independent experiments. *A.U.,* arbitrary units.

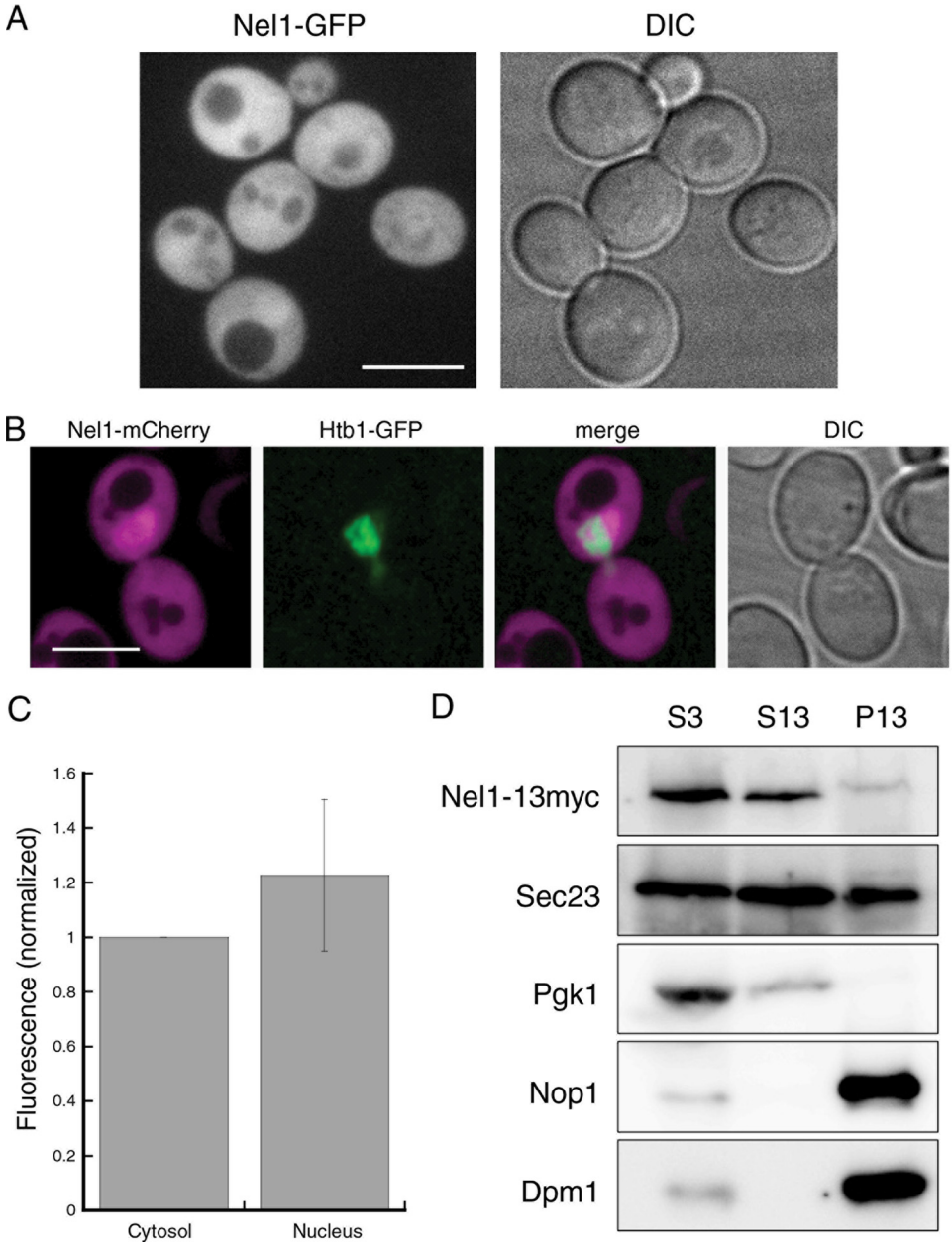

FIGURE 5. **Subcellular localization of Nel1.** *A,* live cell imaging of Nel1-GFP. The cells expressing Nel1-GFP were grown to mid-log phase and observed by confocal microscopy. *B,* Nel1 is localized in the cytosol and the nucleus. The cells expressing Htb1-GFP and Nel1-mCherry were grown to mid-log phase and observed by confocal microscopy. *Scale bars,* 5 μm. *C,* quantification of Nel1 accumulation in the nucleus. The fluorescence intensity of Nel1-GFP was measured, and the ratio of nuclear fluorescence to cytosolic signal was calculated for each cell (normalized relative to the cytosol). The mean $\pm$ S.D. are shown in the *graph*. We counted 80 cells. *D,* subcellular fractionation analyses of Nel1 and Sec23. The CKY1 cells expressing Nel1–13Myc were grown to mid-log phase, converted to spheroplasts, homogenized, and centrifuged at 13,000 $\times$ *g*. The total homogenate (*S3*), supernatant (*S13*), and pellet (*P13*) fractions were analyzed by SDS-PAGE and immunoblotting. The results shown are typical and representative of at least three independent experiments. *DIC*, differential interference contrast.

GFP (36, 37), and in most cells the nuclear signal was slightly stronger (signal ratio of nucleus/cytosol = 1.2 $\pm$ 0.28) (Fig. 5*C*). To evaluate whether the localization pattern of overexpressed Nel1 corresponds to that of endogenous Nel1, we used subcellular fractionation to examine the localization of a C-terminally 13Myc-tagged version of Nel1 (Nel1–13Myc) expressed from its own promoter (Fig. 5*D*). Cells expressing Nel1–13Myc were converted into spheroplasts and homogenized, and the extracts were separated by centrifugation into low speed supernatant (S13) and low speed pellet (P13) fractions (Fig. 5*D*) (28). Under these conditions, the ER membrane marker Dpm1 and the nuclear marker Nop1 were found solely in the P13 fraction. The soluble marker protein Pgk1 was detected exclusively in the S13 fraction, indicating complete cell lysis. A significant portion of Sec23 was recovered in the S13 fraction (percent ratio of P13/total = 62.3 $\pm$ 3.3%), but it was also present in the P13 fraction (percent ratio of P13/total = 37.7 $\pm$ 3.3%), which reflected the amount of Sec23 localized to the ERES (Fig. 5*D*). In contrast, Nel1–13Myc was found to be predominantly localized to the S13 fraction (percent ratio of P13/total = 87.1 $\pm$ 10.0%), and ~3-fold less Nel1–13Myc compared with that of Sec23 was recovered in the P13 fraction (percent ratio of P13/total =

12.9 ± 10.0%) (Fig. 5*D*), which correlates with the localization of the overexpressed Nel1-mCherry we observed via fluorescence microscopy (Fig. 5, *A* and *B*). Together, these findings indicate that Nel1 is predominantly a cytosolic protein and does not accumulate at ERES.

DISCUSSION

Sec23 is commonly known as a component of the COPII coat and also as a GAP for Sar1 that regulates COPII assembly. Here, we showed that the Sec23 homolog Nel1 also has Sar1-GAP activity but lacks the ability to function as a subunit of the COPII coat. Whether the presence of a Nel1-like molecule is specific to *S. cerevisiae* or more widespread among other organisms is currently unclear. However, because several alternative splice variants of the Sec23 gene have been predicted to exist in many higher eukaryotes (Aceview, NCBI), it is possible that one of these variants has the potential to encode a protein with properties similar to those of Nel1.

At the subcellular level, Nel1 was found to be predominantly localized throughout the cytosol, which permits the activation of Sar1 GTPase on the ER membrane. Although overexpression of Sec23 alone has been shown to impair cell growth, we were unable to detect any apparent growth defect when Nel1 was overexpressed. This is likely because Nel1 does not associate with any of the COPII coat components; therefore, it may not compete for COPII coat assembly. In fact, the fluorescence signal of Nel1-mCherry was not concentrated at ERES. To our knowledge, failure to localize at ERES has not previously been described for Sec23 or any of its homologs found in other species (21, 38–40). Although there remains the possibility that the overexpression of Nel1 might affect its normal intracellular localization pattern, our data indicate that Nel1 is also localized in the nucleus. The size limit for passive diffusion through the nuclear pore complex is approximately ~40 kDa (41); therefore, Nel1-mCherry (99 kDa), as well as endogenous Nel1 (72 kDa), are considered too large to diffuse freely into the nucleus. Thus, a functional nuclear localization signal would be required for the active transport of Nel1 into the nucleus; however, no conventional nuclear localization signal is evident in the Nel1 sequence. The exact sequences responsible for nuclear targeting of Nel1 remain to be established.

We further showed here that Nel1 interacts biochemically with Sar1 and acts as a GAP to stimulate GTPase activity. The demonstration that Nel1 binds to the membrane via the GTP-bound form of Sar1 and catalyzes its inactivation implies that Nel1 modulates the activity of Sar1 on the membrane. On the basis of our result that a subpopulation of Nel1 shuttles to the nucleus, it might be possible that Nel1 has a physiological function there. A fraction of Sar1 might also be localized inside the nucleus because endogenous Sar1 (at 21.5 kDa) is small enough to diffuse into the nucleus without requiring a functional nuclear localization signal. Although our genetic analysis of the *nel1*Δ *sar1D32G* double mutant suggests a functional link between Nel1 and Sar1 *in vivo*, further studies will be needed to determine the precise mechanistic relationship between Sar1 and the nucleus-localized Nel1.

To summarize, we identified Nel1 as a novel paralog of Sec23 that has genetic and biochemical interactions with Sar1 in *S. cerevisiae*. The function of Nel1 is currently unknown. However, considering its considerably lower level of expression than that of Sec23, we think it is unlikely that Nel1 functions as a structural component of the vesicle coat machinery. Instead, we propose that Nel1 functions as a signaling molecule. Further investigation may provide insight into the physiological relevance of Sar1/Nel1 function in the cells.

Acknowledgments—We are grateful to the members of the Sato laboratory for helpful discussions.

REFERENCES

1. Barlowe, C. K., and Miller, E. A. (2013) Secretory protein biogenesis and traffic in the early secretory pathway. *Genetics* **193,** 383–410
2. Brandizzi, F., and Barlowe, C. (2013) Organization of the ER-Golgi interface for membrane traffic control. *Nat. Rev. Mol. Cell Biol.* **14,** 382–392
3. D'Arcangelo, J. G., Stahmer, K. R., and Miller, E. A. (2013) Vesicle-mediated export from the ER: COPII coat function and regulation. *Biochim. Biophys. Acta* **1833,** 2464–2472
4. Nakańo, A., and Muramatsu, M. (1989) A novel GTP-binding protein, Sar1p, is involved in transport from the endoplasmic reticulum to the Golgi apparatus. *J. Cell Biol.* **109,** 2677–2691
5. Barlowe, C., d'Enfert, C., and Schekman, R. (1993) Purification and characterization of SAR1p, a small GTP-binding protein required for transport vesicle formation from the endoplasmic reticulum. *J. Biol. Chem.* **268,** 873–879
6. Barlowe, C., Orci, L., Yeung, T., Hosobuchi, M., Hamamoto, S., Salama, N., Rexach, M. F., Ravazzola, M., Amherdt, M., and Schekman, R. (1994) COPII: a membrane coat formed by Sec proteins that drive vesicle budding from the endoplasmic reticulum. *Cell* **77,** 895–907
7. Nakano, A., Brada, D., and Schekman, R. (1988) A membrane glycoprotein, Sec12p, required for protein transport from the endoplasmic reticulum to the Golgi apparatus in yeast. *J. Cell Biol.* **107,** 851–863
8. Barlowe, C., and Schekman, R. (1993) SEC12 encodes a guanine-nucleotide-exchange factor essential for transport vesicle budding from the ER. *Nature* **365,** 347–349
9. Bi, X., Corpina, R. A., and Goldberg, J. (2002) Structure of the Sec23/24-Sar1 pre-budding complex of the COPII vesicle coat. *Nature* **419,** 271–277
10. Mossessova, E., Bickford, L. C., and Goldberg, J. (2003) SNARE selectivity of the COPII coat. *Cell* **114,** 483–495
11. Miller, E. A., Beilharz, T. H., Malkus, P. N., Lee, M. C., Hamamoto, S., Orci, L., and Schekman, R. (2003) Multiple cargo binding sites on the COPII subunit Sec24p ensure capture of diverse membrane proteins into transport vesicles. *Cell* **114,** 497–509
12. Bi, X., Mancias, J. D., and Goldberg, J. (2007) Insights into COPII coat nucleation from the structure of Sec23.Sar1 complexed with the active fragment of Sec31. *Dev. Cell* **13,** 635–645
13. Tabata, K. V., Sato, K., Ide, T., Nishizaka, T., Nakano, A., and Noji, H. (2009) Visualization of cargo concentration by COPII minimal machinery in a planar lipid membrane. *EMBO J.* **28,** 3279–3289
14. Yoshihisa, T., Barlowe, C., and Schekman, R. (1993) Requirement for a GTPase-activating protein in vesicle budding from the endoplasmic reticulum. *Science* **259,** 1466–1468
15. Antonny, B., Madden, D., Hamamoto, S., Orci, L., and Schekman, R. (2001) Dynamics of the COPII coat with GTP and stable analogues. *Nat. Cell Biol.* **3,** 531–537
16. Futai, E., Hamamoto, S., Orci, L., and Schekman, R. (2004) GTP/GDP exchange by Sec12p enables COPII vesicle bud formation on synthetic liposomes. *EMBO J.* **23,** 4146–4155
17. Sato, K., and Nakano, A. (2005) Dissection of COPII subunit-cargo assembly and disassembly kinetics during Sar1p-GTP hydrolysis. *Nat. Struct. Mol. Biol.* **12,** 167–174
18. Kung, L. F., Pagant, S., Futai, E., D'Arcangelo, J. G., Buchanan, R., Dittmar, J. C., Reid, R. J., Rothstein, R., Hamamoto, S., Snapp, E. L., Schekman, R.,

and Miller, E. A. (2012) Sec24p and Sec16p cooperate to regulate the GTP cycle of the COPII coat. *EMBO J.* **31,** 1014–1027
19. Yorimitsu, T., and Sato, K. (2012) Insights into structural and regulatory roles of Sec16 in COPII vesicle formation at ER exit sites. *Mol. Biol. Cell* **23,** 2930–2942
20. Miller, E. A., and Schekman, R. (2013) COPII-a flexible vesicle formation system. *Curr. Opin. Cell Biol.* **25,** 420–427
21. Paccaud, J. P., Reith, W., Carpentier, J. L., Ravazzola, M., Amherdt, M., Schekman, R., and Orci, L. (1996) Cloning and functional characterization of mammalian homologues of the COPII component Sec23. *Mol. Biol. Cell* **7,** 1535–1546
22. Gueldener, U., Heinisch, J., Koehler, G. J., Voss, D., and Hegemann, J. H. (2002) A second set of loxP marker cassettes for Cre-mediated multiple gene knockouts in budding yeast. *Nucleic Acids Res.* **30,** e23
23. Saito, Y., Yamanushi, T., Oka, T., and Nakano, A. (1999) Identification of SEC12, SED4, truncated SEC16, and EKS1/HRD3 as multicopy suppressors of ts mutants of Sar1 GTPase. *J. Biochem.* **125,** 130–137
24. James, P., Halladay, J., and Craig, E. A. (1996) Genomic libraries and a host strain designed for highly efficient two-hybrid selection in yeast. *Genetics* **144,** 1425–1436
25. Longtine, M. S., McKenzie, A., 3rd, Demarini, D. J., Shah, N. G., Wach, A., Brachat, A., Philippsen, P., and Pringle, J. R. (1998) Additional modules for versatile and economical PCR-based gene deletion and modification in *Saccharomyces cerevisiae*. *Yeast* **14,** 953–961
26. Matsuoka, K., and Schekman, R. (2000) The use of liposomes to study COPII- and COPI-coated vesicle formation and membrane protein sorting. *Methods* **20,** 417–428
27. Matsuoka, K., Orci, L., Amherdt, M., Bednarek, S. Y., Hamamoto, S., Schekman, R., and Yeung, T. (1998) COPII-coated vesicle formation reconstituted with purified coat proteins and chemically defined liposomes. *Cell* **93,** 263–275
28. Vida, T. A., Graham, T. R., and Emr, S. D. (1990) *In vitro* reconstitution of intercompartmental protein transport to the yeast vacuole. *J. Cell Biol.* **111,** 2871–2884
29. Novick, P., Field, C., and Schekman, R. (1980) Identification of 23 complementation groups required for post-translational events in the yeast secretory pathway. *Cell* **21,** 205–215
30. Kurihara, T., Hamamoto, S., Gimeno, R. E., Kaiser, C. A., Schekman, R., and Yoshihisa, T. (2000) Sec24p and Iss1p function interchangeably in transport vesicle formation from the endoplasmic reticulum in *Saccharomyces cerevisiae*. *Mol. Biol. Cell* **11,** 983–998
31. Roberg, K. J., Crotwell, M., Espenshade, P., Gimeno, R., and Kaiser, C. A. (1999) LST1 is a SEC24 homologue used for selective export of the plasma membrane ATPase from the endoplasmic reticulum. *J. Cell Biol.* **145,** 659–672
32. Shimoni, Y., Kurihara, T., Ravazzola, M., Amherdt, M., Orci, L., and Schekman, R. (2000) Lst1p and Sec24p cooperate in sorting of the plasma membrane ATPase into COPII vesicles in *Saccharomyces cerevisiae*. *J. Cell Biol.* **151,** 973–984
33. Yamanushi, T., Hirata, A., Oka, T., and Nakano, A. (1996) Characterization of yeast sar1 temperature-sensitive mutants, which are defective in protein transport from the endoplasmic reticulum. *J. Biochem.* **120,** 452–458
34. Rossanese, O. W., Soderholm, J., Bevis, B. J., Sears, I. B., O'Connor, J., Williamson, E. K., and Glick, B. S. (1999) Golgi structure correlates with transitional endoplasmic reticulum organization in *Pichia pastoris* and *Saccharomyces cerevisiae*. *J. Cell Biol.* **145,** 69–81
35. Shindiapina, P., and Barlowe, C. (2010) Requirements for transitional endoplasmic reticulum site structure and function in *Saccharomyces cerevisiae*. *Mol. Biol. Cell* **21,** 1530–1545
36. Michelsen, K., Mrowiec, T., Duderstadt, K. E., Frey, S., Minor, D. L., Mayer, M. P., and Schwappach, B. (2006) A multimeric membrane protein reveals 14-3-3 isoform specificity in forward transport in yeast. *Traffic* **7,** 903–916
37. Zou, S., Liu, Y., Zhang, X. Q., Chen, Y., Ye, M., Zhu, X., Yang, S., Lipatova, Z., Liang, Y., and Segev, N. (2012) Modular TRAPP complexes regulate intracellular protein trafficking through multiple Ypt/Rab GTPases in *Saccharomyces cerevisiae*. *Genetics* **191,** 451–460
38. Orci, L., Ravazzola, M., Meda, P., Holcomb, C., Moore, H. P., Hicke, L., and Schekman, R. (1991) Mammalian Sec23p homologue is restricted to the endoplasmic reticulum transitional cytoplasm. *Proc. Natl. Acad. Sci. U.S.A.* **88,** 8611–8615
39. Yang, Y. D., Elamawi, R., Bubeck, J., Pepperkok, R., Ritzenthaler, C., and Robinson, D. G. (2005) Dynamics of COPII vesicles and the Golgi apparatus in cultured *Nicotiana tabacum* BY-2 cells provides evidence for transient association of Golgi stacks with endoplasmic reticulum exit sites. *Plant Cell* **17,** 1513–1531
40. Esaki, M., Liu, Y., and Glick, B. S. (2006) The budding yeast *Pichia pastoris* has a novel Sec23p homolog. *FEBS Lett.* **580,** 5215–5221
41. Terry, L. J., Shows, E. B., and Wente, S. R. (2007) Crossing the nuclear envelope: hierarchical regulation of nucleocytoplasmic transport. *Science* **318,** 1412–1416